

Three-dimensional electromagnetic breathers in carbon nanotubes with the field inhomogeneity along their axes

Alexander V. Zhukov, Roland Bouffanais, Eduard G. Fedorov, and Mikhail B. Belonenko

Citation: *J. Appl. Phys.* **114**, 143106 (2013); doi: 10.1063/1.4824370

View online: <http://dx.doi.org/10.1063/1.4824370>

View Table of Contents: <http://jap.aip.org/resource/1/JAPIAU/v114/i14>

Published by the AIP Publishing LLC.

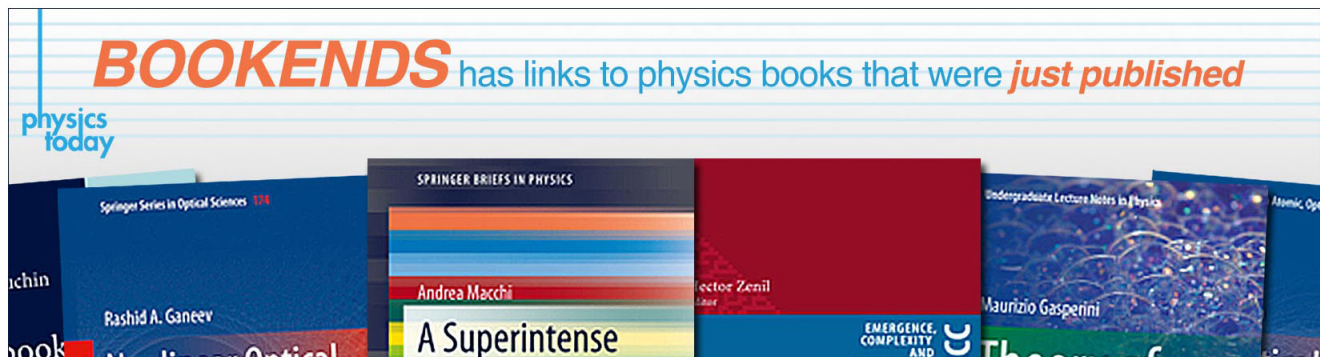
Additional information on J. Appl. Phys.

Journal Homepage: <http://jap.aip.org/>

Journal Information: http://jap.aip.org/about/about_the_journal

Top downloads: http://jap.aip.org/features/most_downloaded

Information for Authors: <http://jap.aip.org/authors>



Three-dimensional electromagnetic breathers in carbon nanotubes with the field inhomogeneity along their axes

Alexander V. Zhukov,^{1,a)} Roland Bouffanais,¹ Eduard G. Fedorov,² and Mikhail B. Belonenko³

¹Singapore University of Technology and Design, 20 Dover Drive, 138682, Singapore

²Volgograd State University of Architecture and Civil Engineering, 400074 Volgograd, Russia

³Laboratory of Nanotechnology, Volgograd Institute of Business, 400048 Volgograd, Russia

(Received 25 July 2013; accepted 20 September 2013; published online 11 October 2013)

We study the propagation of extremely short electromagnetic three-dimensional bipolar pulses in an array of semiconductor carbon nanotubes. The heterogeneity of the pulse field along the axis of the nanotubes is accounted for the first time. The evolution of the electromagnetic field and the charge density of the sample are described by Maxwell's equations supplemented by the continuity equation. Our analysis reveals for the first time the possibility of propagation of three-dimensional electromagnetic breathers in CNTs arrays. Specifically, we found that the propagation of short electromagnetic pulse induces a redistribution of the electron density in the sample. © 2013 AIP Publishing LLC. [<http://dx.doi.org/10.1063/1.4824370>]

I. INTRODUCTION

Carbon nanotubes (CNTs) are considered as one of the most promising building blocks in modern nanoelectronics.¹ Among their very many peculiar features, the nonlinearity of the electron dispersion in nanotubes leads to a wide range of properties, which manifest in fields of moderate intensity $\sim 10^3 - 10^5$ V/cm (see, e.g., Refs. 2 and 3, and references therein). Recent successes of laser physics in the generation of powerful electromagnetic radiations with given parameters⁴ have provided the impetus for comprehensive studies of electronic and optical properties of CNTs in the presence of an electromagnetic field. In this regard, a series of papers⁵⁻¹⁰ has been devoted to studies of the propagation of extremely short electromagnetic pulses in an array of CNTs. In particular, the possibility for propagation of solitary electromagnetic waves in an array of CNTs has been demonstrated, as well as the dynamics of a periodic train of electromagnetic pulses, and the induced current domains have been investigated.

It should be noted that both theoretical and experimental studies of electromagnetic solitary waves have a rather long history. In particular, in the last two decades, optical solitons in Bose-Einstein condensates have attracted a growing body of interest (see Ref. 11 for a review on this topic). More generally, the propagation of stable/quasistable optical solitons requires specific types of medium nonlinearity. The latter can be provided, e.g., by a proper choice of nonlinear lattices (topic comprehensively reviewed in Ref. 12). In this context, the CNT arrays provide one of the unique and practically reliable systems for studying various aspects of nonlinear electromagnetic waves propagation in media.

In spite of their obvious success, a number of issues related to wave propagation in CNTs still remain and require further investigation. That could potentially reveal new effects that may be of interest from a practical point of view. In particular, there are certain questions related to going

beyond the canonical two-dimensional (2D) modeling framework, and taking into account three-dimensional (3D) effects such as, for instance, the transverse dispersion in a study of the dynamics of electromagnetic waves. For example, the possibility of the propagation of cylindrically symmetric electromagnetic waves in an array of nanotubes has been demonstrated.¹³ The possibility of the propagation of 2D traveling solitary electromagnetic waves (a.k.a. *light bullets*) has been demonstrated and reported in Ref. 14. Subsequently, their interaction with inhomogeneities in the arrays of nanotubes has been investigated.¹⁵⁻¹⁷ The possibility of propagation of 2D bipolar electromagnetic pulses in semiconductor arrays of CNTs is revealed in Ref. 18. Recently, the authors considered also the general aspects of stability of the laser beams propagating in an array of CNTs.¹⁹

It should be noted that the theoretical analysis in the abovementioned studies has been performed under the assumption of homogeneity of the pulse field along the axis of the CNTs. However, the heterogeneity of this field can cause the emergence of interesting and unexpected physical effects of potentially practical importance. In particular, Ref. 20 is concerned with the 2D model of the propagation of ultrashort electromagnetic pulses in an array of CNTs with the heterogeneity of the field along their axis. As a result, it was found that in that specific case, an electromagnetic pulse induces a significant redistribution of the electron density in the sample. In spite of the interesting theoretical outcome of that research, the 2D approximation makes an experimental realization hardly feasible.

In this context, it seems timely to devise and study the 3D model of the propagation of laser pulses in an array of semiconductor CNTs with the spatial inhomogeneity of the pulse field along the axis of the nanotubes. To that aim, the formulation of the problem must involve the construction of a model in which the evolution of electromagnetic waves is space limited in all three directions of the Cartesian coordinates system. The solution of this problem opens the door to the study of problems in which we could consider the field

^{a)}Electronic mail: alex_zhukov@sutd.edu.sg

generated by the substrate onto which the CNTs were grown. The relevance of this range of issues is evident in the light of a number of prospective tasks in modern optoelectronics.

II. BASIC RELATIONS AND THE WAVE EQUATION

Let us consider the following particular setup, consisting of the propagation of a laser pulse through the bulk semiconductor array of single-walled CNTs of the *zigzag* type, $(m, 0)$, where the number m determines the radius of the nanotube through $R = \sqrt{3}bm/2\pi$, with b the distance between nearest-neighbor carbon atoms.³ Note that our choice of CNTs is primarily guided by the presence of stable solitary solutions even for a generic sine-Gordon case in 2D.²¹ Furthermore, we assume that the nanotubes are placed into a homogeneous insulator in a way that the axes of the nanotubes are parallel to the common Ox -axis, and the distances between neighboring nanotubes are large compared to their diameter. This specific assumption allows us to neglect the interaction between CNTs.

Essentially, the chosen geometry of the problem is similar to the one considered in Ref. 18, except for the fact that in the present study, all the quantities are assumed to be 3D-spatially dependent. Given the above framework, the dispersion relation for the conduction electrons of CNTs takes the form

$$\Delta(p_x, s) = \gamma_0 \left\{ 1 + 4\cos\left(p_x \frac{d_x}{\hbar}\right) \cos\left(\pi \frac{s}{m}\right) + 4\cos^2\left(\pi \frac{s}{m}\right) \right\}^{1/2}, \quad (1)$$

where the quasimomentum is represented as $\mathbf{p} = \{p_x, s\}$, with $s = 1, 2, \dots, m$ is the number characterizing the momentum quantization along the perimeter of the nanotube, γ_0 is the overlap integral, and $d_x = 3b/2$.^{2,3}

For definiteness, we consider the propagation of a laser beam in an array of CNTs in the direction perpendicular to their axes, namely along the Oz -axis with our choice of spatial coordinates. Further, we assume that the electric field of the laser beam, $\mathbf{E} = \{E(x, y, z, t), 0, 0\}$, is oriented along the Ox -axis. The characteristic pulse duration τ_p is supposed to satisfy the condition $\tau_p \ll \tau_{rel}$, where τ_{rel} is the characteristic relaxation time. The latter condition allows us to use the collisionless approximation to describe the evolution of the pulse field.⁵

The electromagnetic field in an array of nanotubes can be described by Maxwell's equations,²³ which in our case read

$$\frac{\varepsilon}{c^2} \frac{\partial^2 \mathbf{A}}{\partial t^2} - \frac{\partial^2 \mathbf{A}}{\partial x^2} - \frac{\partial^2 \mathbf{A}}{\partial y^2} - \frac{\partial^2 \mathbf{A}}{\partial z^2} - \frac{4\pi}{c} \mathbf{j} = 0. \quad (2)$$

Here $A(x, y, z, t)$ and $j(x, y, z, t)$ are the projections of the vector potential $\mathbf{A} = (A, 0, 0)$ and the current density $\mathbf{j} = (j, 0, 0)$ onto the Ox -axis, ε is the permittivity of the medium, and c is the speed of light in vacuum. The electric field of the laser beam is determined by the gauge condition $c\mathbf{E} = -\partial\mathbf{A}/\partial t$.²⁴

We find the conduction current density in an array following the approach developed in Refs. 18, 19, and 25.

Representing the electron energy spectrum (1) as a Fourier series, we write the expression for the projection of the current density on the Ox -axis in the collisionless approximation, namely

$$j = -en \frac{d_x}{\hbar} \gamma_0 \sum_{s=1}^m \sum_{r=1}^{\infty} G_{r,s} \sin \left\{ er \frac{d_x}{\hbar} \left(\frac{A}{c} + \int_0^t \frac{\partial \phi}{\partial x} dt \right) \right\}, \quad (3)$$

where e is the electron charge, n is the concentration of conduction electrons in the array of nanotubes, and ϕ is the scalar potential of electric field. The coefficients $G_{r,s}$ appearing in Eq. (3) are explicitly given by

$$G_{r,s} = -r \frac{\delta_{r,s}}{\gamma_0} \frac{\int_{-\pi}^{\pi} \cos(r\alpha) \exp \left\{ -\sum_{r=1}^{\infty} \theta_{r,s} \cos(r\alpha) \right\} d\alpha}{\int_{-\pi}^{\pi} \exp \left\{ -\sum_{r=1}^{\infty} \theta_{r,s} \cos(r\alpha) \right\} d\alpha}, \quad (4)$$

with $\theta_{r,s} = \delta_{r,s} (k_B T)^{-1}$, and $\delta_{r,s}$ are the coefficients in the expansion of the spectrum (1) in a Fourier series, namely

$$\delta_{r,s} = \frac{d_x}{\pi \hbar} \int_{-\pi \hbar/d_x}^{\pi \hbar/d_x} \Delta(p_x, s) \cos \left(r \frac{d_x}{\hbar} p_x \right) dp_x. \quad (5)$$

The current density in Eq. (3) explicitly depends on the potentials \mathbf{A} and ϕ . Therefore, it might be assumed that the change of the vector potential by adding a scalar constant (which is classically known not to lead to any physical consequence) causes a change in the current density. However, in reality, this does not happen, because while deriving Eq. (3), it was assumed that the potentials \mathbf{A} and ϕ initially (at $t=0$) are zero valued, which fixes their choice. Substituting the expression for the conduction current Eq. (3) into Eq. (2) yields the desired wave equation describing the evolution of the field in the array of CNTs

$$\frac{\partial^2 \Psi}{\partial \tau^2} - \left(\frac{\partial^2 \Psi}{\partial \xi^2} + \frac{\partial^2 \Psi}{\partial \nu^2} + \frac{\partial^2 \Psi}{\partial \zeta^2} \right) + \eta \sum_{s=1}^m \sum_{r=1}^{\infty} G_{r,s} \sin \left\{ r \left(\Psi + \int_0^{\tau} \frac{\partial \Phi}{\partial \xi} d\tau \right) \right\} = 0. \quad (6)$$

Here $\Psi = Aed_x/c\hbar$ is the dimensionless projection of the vector potential on the Ox -axis; $\Phi = \phi ed_x/c\hbar$; $\tau = \omega_0 t/\sqrt{\varepsilon}$ is the dimensionless time; $\xi = x\omega_0/c$, $\nu = y\omega_0/c$ and $\zeta = z\omega_0/c$ are the dimensionless coordinates; $\eta = n/n_0$, where n_0 is the equilibrium electron concentration in the absence of external fields; and ω_0 is the characteristic frequency, defined by the formula

$$\omega_0 = 2 \frac{|e|d_x}{\hbar} \sqrt{\pi \gamma_0 n_0}. \quad (7)$$

As stated earlier, we assume that the electric field is non-uniform along the direction parallel to the Ox -axis, which may result into a charge density redistribution. Since the total charge stored in the sample is conserved, the distribution in the charge density is determined by the continuity equation

$$\frac{\partial j}{\partial x} + \frac{\partial \rho}{\partial t} = 0, \quad (8)$$

where $\rho = |e|n_0\eta$ is the volume density of charge. By substituting Eq. (3) into Eq. (8), we obtain the equation describing the evolution of the charge density caused by the electromagnetic pulse field,

$$\frac{\partial \eta}{\partial \tau} = \frac{\gamma_0 d_x \sqrt{\varepsilon}}{c \hbar} \sum_{s=1}^m \sum_{r=1}^{\infty} G_{r,s} \frac{\partial}{\partial \xi} \left\{ \eta \sin \left[r \left(\Psi + \int_0^\tau \frac{\partial \Phi}{\partial \xi} d\tau \right) \right] \right\}. \quad (9)$$

The redistribution of the electron density is accompanied by a change in the distribution of the scalar field potential in the system. Maxwell's equations^{23,24} lead to the following relation for the scalar potential:

$$\frac{\partial^2 \Phi}{\partial \tau^2} - \left(\frac{\partial^2 \Phi}{\partial \xi^2} + \frac{\partial^2 \Phi}{\partial \nu^2} + \frac{\partial^2 \Phi}{\partial \zeta^2} \right) = \beta(\eta - 1), \quad (10)$$

where $\beta = c\hbar/\varepsilon\gamma_0 d_x$. Thus, the evolution of the field in the system with the charge density redistribution is defined by the set of Eqs. (6), (9), and (10). The electric field of the wave in this array of nanotubes, given its form $\mathbf{E} = (E, 0, 0)$, reads

$$E = -\frac{1}{c} \frac{\partial A}{\partial t} = E_0 \frac{\partial \Psi}{\partial \tau}, \quad (11)$$

in which E_0 is given by

$$E_0 = -\frac{\hbar\omega_0}{ed_x\sqrt{\varepsilon}}. \quad (12)$$

As is well known, the practically measurable physical quantities are the intensity, energy, or power of the electromagnetic radiation, which are proportional to the square of the absolute value of the electric field vector.²³ Taking into account the expression (11) and the chosen gauge for a vector potential, the intensity $I = |\mathbf{E}|^2$ takes the form

$$I = I_0 \left(\frac{\partial \Psi}{\partial \tau} \right)^2, \quad (13)$$

where $I_0 = E_0^2$ (see Eq. (12)).

III. NUMERICAL SIMULATION AND THE DISCUSSION OF RESULTS

The system of governing Eqs. (6), (9), and (10) in general does not possess any exact analytical solutions. Hence, we carried out a numerical study of the propagation of an electromagnetic pulse in an array of CNTs. To make a proper choice of initial conditions, it is important keeping in mind the following considerations: Eq. (6) can be considered as a generalization of the classical sine-Gordon equation to the 3D case, where the generalized potential is expanded as a Fourier series. The numerical calculations show that the coefficients $G_{r,s}$ decrease rapidly with increasing r , i.e.,

$|G_{1,s}| \gg |G_{2,s}|$, etc. Restricting ourselves to the one-dimensional approximation and considering only the first leading term in the sum over r in Eq. (6), we are able to arrive at the sine-Gordon equation in a form relatively close to its canonical one, which admits *breathers* as solutions.²⁶ Note that the possibility of propagation of breathers in solids, and in particular, in semiconductor superlattices (one-dimensional model), was theoretically predicted earlier.²⁷ Thus, it is natural to assume that the system described by Eq. (6) allows the propagation of bipolar solitary waves similar to breathers of the sine-Gordon equation.

We assume that at time $\tau = 0$, the array of CNTs is irradiated by an electromagnetic pulse of a breather structure, whose dimensionless vector potential has the form

$$\Psi = 4 \arctan \left\{ \frac{\sin \chi}{\cosh \mu} \sqrt{\frac{1}{\Omega^2} - 1} \right\} \exp \left\{ -\left(\frac{\xi - \xi_0}{\lambda_\xi} \right)^2 \right\} \times \exp \left\{ -\left(\frac{\nu - \nu_0}{\lambda_\nu} \right)^2 \right\}, \quad (14)$$

where we have used the following notations:

$$\chi = \Omega \frac{\tau - (\zeta - \zeta_0)u/v}{\sqrt{1 - (u/v)^2}}, \quad (15)$$

$$\mu = \{ \tau u/v - (\zeta - \zeta_0) \} \sqrt{\frac{1 - \Omega^2}{1 - (u/v)^2}}, \quad (16)$$

$\Omega = \omega_B/\omega_0$ is the parameter determined by the natural frequency of the breather ω_B ($\Omega < 1$); u/v is the ratio of the pulse velocity u to the speed of light in the medium $v = c/\sqrt{\varepsilon}$; ξ_0 , ν_0 and ζ_0 are the dimensionless coordinates along the Ox -, Oy -, and Oz -axes, respectively, at $\tau = 0$; λ_ξ and λ_ν are the dimensionless half-widths of the pulse along the Ox - and Oy -axis, respectively.

The electric field of an electromagnetic pulse in an array is determined by Eq. (11) with Ψ given by Eq. (14). The first factor in Eq. (14) is a traveling breather, propagating with velocity u . The presence of the second and third factors of the Gaussian form in Eq. (14) is dictated by the fact that the Gaussian intensity distribution is of great interest from an applied point of view in different fields of physics and engineering. This is due to the minimum of the diffraction spreading of Gaussian beams, where such beams are very close to reality.¹⁹

We also assume that at the initial instant $\tau = 0$, the electron density n is equal to n_0 , and the scalar potential ϕ is zero, so that we have the initial conditions

$$\eta(\xi, \nu, \zeta, \tau) = 1, \quad (17)$$

$$\Phi(\xi, \nu, \zeta, \tau) = 0. \quad (18)$$

For the numerical solution of the set of Eqs. (6), (9) and (10), together with the initial conditions (14), (17), and (18), we have implemented explicit finite-difference schemes for the hyperbolic equations.²⁸ The obtained values of $\Psi(\xi, \nu, \zeta, \tau)$ have been further used to calculate the electric

field by means of Eq. (11), as well as the intensity distribution of the field through Eq. (13). We also calculated the distribution of the quantity $\eta = \eta(\xi, \nu, \zeta, \tau)$, which determines the electron concentration in the sample through $n = \eta n_0$.

In the present study, we have used the following realistic physical parameters: $m = 7$, $\gamma_0 = 2.7$ eV, $b = 1.42 \times 10^{-8}$ cm, $d_x \approx 2.13 \times 10^{-8}$ cm, $n_0 = 2 \times 10^{18}$ cm $^{-3}$,²² $T = 77$ K, $\varepsilon = 4$, and $\omega_0 \approx 10^{14}$ s $^{-1}$ (see Eq. (7)). Note that the collisionless approximation used in this study is justified when considering processes at times not exceeding the relaxation time $t_{\text{rel}} \approx 3 \times 10^{-13}$ s.² Indeed during this time, light in this medium travels the distance $z = ct_{\text{rel}}/\sqrt{\varepsilon} \approx 10^{-2}$ cm.

Figures 1–3 show our results for the modeling of the bipolar laser pulses in an array of CNTs. For definiteness, the following initial parameters were used: $u/v = 0.9$ (which corresponds to the breather speed $u = 1.35 \times 10^{10}$ cm/s), $\Omega = 0.5$ (equivalent to $\omega_B = \Omega\omega_0 \approx 5.05 \times 10^{13}$ s $^{-1}$), and

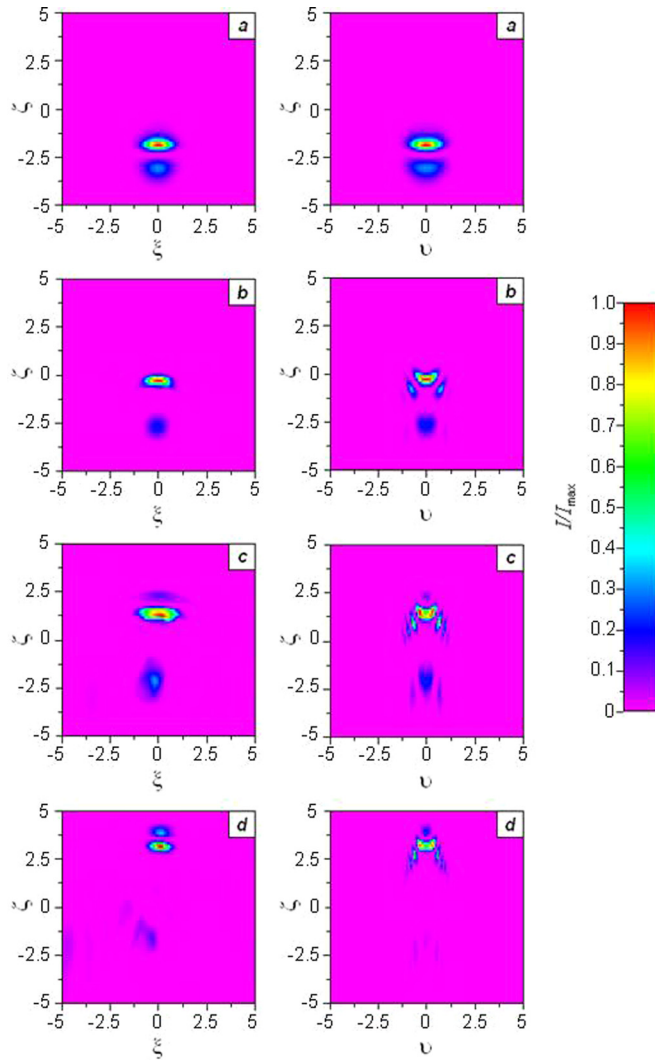


FIG. 1. Field intensity distribution in the array of CNTs in planes $\xi O \xi \zeta$ (for $\nu = \nu_0$) and $\nu O \xi \zeta$ (for $\xi = \xi_0$) at different points of the dimensionless time $\tau = \omega_0 t / \sqrt{\varepsilon}$ during the propagation of laser pulse: (a) $\tau = 0.5$, (b) $\tau = 3.5$, (c) $\tau = 6.5$, (d) $\tau = 9.5$. The axes are scaled using the dimensionless coordinates $\xi = x\omega_0/c$, $\nu = y\omega_0/c$, and $\zeta = z\omega_0/c$. Values of the ratio I/I_{max} are mapped on a color scale, the maximum values of the field intensity correspond to red, and minimum ones to purple. I_{max} is the maximum value of I at the given instant τ considered.

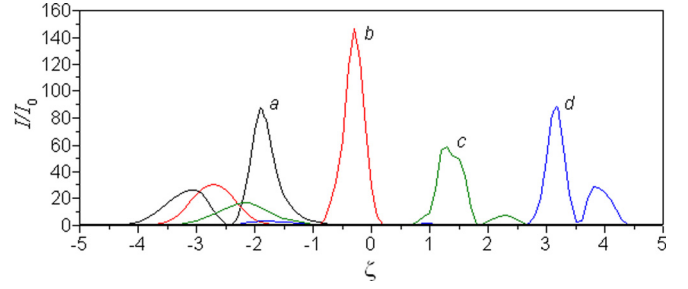


FIG. 2. Intensity distribution $I(\xi_0, \nu_0, \xi, \tau)/I_0$ of the pulse field in an array of CNTs along the line parallel to the axis $O \xi \zeta$ and passing through the point with coordinates $\xi, \nu = \xi_0, \nu_0$, at different instants of the dimensionless time τ : (a) $\tau = 0.5$, (b) $\tau = 3.5$, (c) $\tau = 6.5$, (d) $\tau = 9.5$. The horizontal axis is scaled using the dimensionless coordinate $\xi = z\omega_0/c$.

$\lambda_\xi = \lambda_\nu = 1$ (equivalent to the pulse half-width along the axes Ox and Oy equal to $L_y = L_x = \lambda_\xi c / \omega_0 \approx 3 \times 10^{-4}$ cm).

Figure 1 presents the field intensity distribution in the array of CNTs in the planes $\xi O \xi \zeta$ and $\nu O \xi \zeta$ at different instants of the dimensionless time $\tau = \omega_0 t / \sqrt{\varepsilon}$. The field intensity is represented by the ratio I/I_{max} , different values of which correspond to a variation of colors (flooded contours) with a colormap from violet to red. The quantity I_{max} stands for the maximum intensity at the given instant τ considered. Red areas correspond to near-maximum intensity, while purple ones reflect near-minimum intensity regions. The distribution is plotted using the set of dimensionless coordinates, $\xi = x\omega_0/c$, $\nu = y\omega_0/c$ and $\zeta = z\omega_0/c$. With the parameters selected above, the units on the axes correspond to the following physical distances $\Delta x = \Delta z = \Delta y \approx 3 \times 10^{-4}$ cm. Figure 2 displays the distribution of the intensity of the electromagnetic field pulses in an array of CNTs along a line parallel to the axis $O \xi \zeta$, and passing through the point with coordinates $\xi = \xi_0$ and $\nu = \nu_0$ at the same instants of time as those considered in Figure 1. In other words, Figure 2 allows us to visualize the one-dimensional variations of the pulse shape. The numerical analysis reveals that as the pulse propagates, along with a periodic change in its shape, a periodical change in its amplitude concurrently takes place. Those one-dimensional spatial variations are supplemented by Fig. 3, which shows the time dependence of the maximum intensity I_{max} along a line parallel to the axis $O \xi \zeta$ and passing through the point with coordinates $\xi = \xi_0$ and $\nu = \nu_0$, using the same physical values as the ones used to generate Figs. 1 and 2.

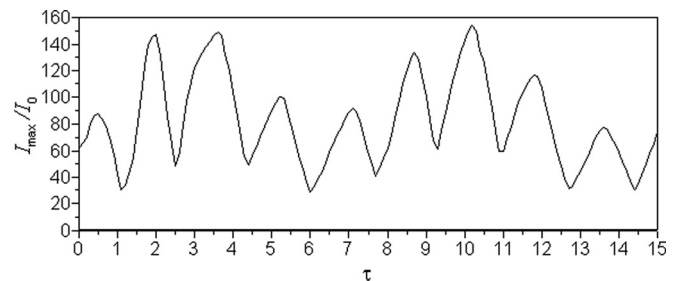


FIG. 3. Dependence of the ratio I_{max}/I_0 on the dimensionless time τ along the line parallel to the axis $O \xi \zeta$ and passing through the point with coordinates $\xi, \nu = \xi_0, \nu_0$. The horizontal axis is scaled using the dimensionless coordinate $\tau = \omega_0 t / \sqrt{\varepsilon}$.

At this point, we would like to pay particular attention to the range of parameters for which our qualitative conclusions apply. The first restriction is related to the time interval considered in our study. As expected from earlier investigations reported in Refs. 2 and 3, the characteristic relaxation time is $t_{\text{rel}} \approx 3 \times 10^{-13}$ s, so that for typical CNTs parameters— $\omega_0 \approx 10^{14} \text{ s}^{-1}$ and $\varepsilon = 4$ —we have $\tau_{\text{rel}} = \omega_0 t_{\text{rel}} / \sqrt{\varepsilon} \approx 15$. For longer times, the collisionless model no longer applies. Hence, our results are strictly valid within the range $\{0; \tau_{\text{rel}}\}$. Another key parameter is the initial velocity of the pulse. We have varied the dimensionless velocity u/v in a range comprised between 0.5 and 0.98. There is actually no sense to consider velocity smaller than 0.5, given that during the time τ_{rel} , our light bullet travels too short a distance—only slightly longer than its own linear size. For $u/v > 0.5$, the bullet travels a fairly significant distance, much larger than its linear size. However, in the present study, we did not go beyond 0.98 due to limitations imposed by our numerical scheme. The dimensionless half-widths λ_ξ and λ_ν are supposed to be of the order of unity. We have tested different values within the range $\{0.5; 1.5\}$ and observed no qualitative difference. Thus, for definiteness, in this paper, we present results for $\lambda_\xi = \lambda_\nu = 1$. Finally, another important parameter is the natural frequency $\Omega = \omega_B / \omega_0$. Keeping in mind the necessary condition $\Omega < 1$, we have analyzed different values and observed stable results in the range $\{0.3; 0.7\}$. Beyond 0.7, the initial width of bullet along its wavevector becomes too large and no longer fits into our computational domain for reliable values of ζ .

The three above figures demonstrate that the three-dimensional electromagnetic pulses propagate in a nanotube array stably, i.e., without incurring substantial spreading and dispersion. Thus, the inhomogeneity of the electric field distribution along the axis of nanotubes does not affect the stability of extremely short pulses, but causes some change in their shape, as compared with the low-dimensional cases. For example, the speed and the shape of a tail formed during the pulse propagation in homogeneous low-dimensional problems are dictated by the imbalance between dispersion and nonlinearity. In our 3D case, a tail appears due to the field inhomogeneity along the nanotubes axis and the charge redistribution within a sample during the pulse propagation. To this aim, Fig. 4 presents the distribution of electron density in the nanotube array as given by $n = \eta n_0$. The electron density is represented by the dimensionless ratio $\tilde{\eta} = (\eta - \eta_{\text{min}}) / (\eta_{\text{max}} - \eta_{\text{min}})$, where η_{max} and η_{min} stand for the maximum and minimum values of η at a given instant τ , respectively. Red areas in Fig. 4 correspond to high electron density zones, whereas purple areas represent low electron density zones. This effect of redistribution of the charge density induced by the passage of the laser pulse may be put, in our opinion, as a basis for the creation and development of chemical sensors based on CNTs. Areas with a high or a low electron density generated by the laser pulse can play the role of an attraction center for ions or polarized molecules contained in the analyzed gas mixtures. Thus, the peculiarities of the propagation of extremely short electromagnetic pulses through an array of CNTs described in this paper can have practical value in designing the element base for modern nanoelectronics.

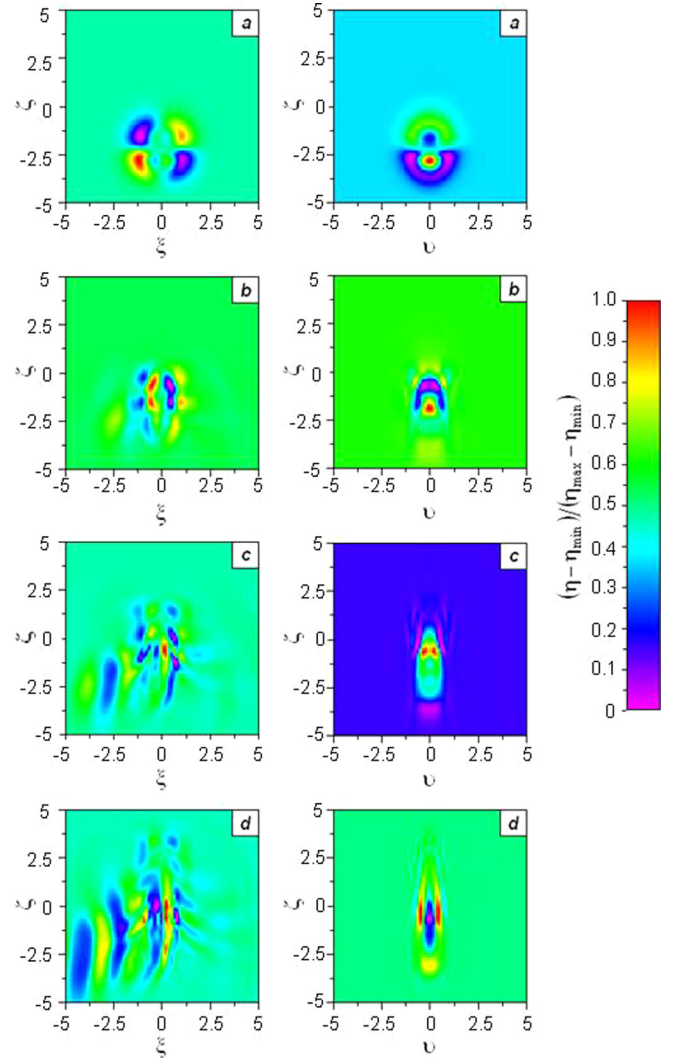


FIG. 4. Electron density distribution in the array of CNTs in the planes $\xi O \xi$ (for $\nu = \nu_0$) and $\nu O \xi$ (for $\xi = \xi_0$) at different points of the dimensionless time $\tau = \omega_0 t / \sqrt{\varepsilon}$ during the propagation of the laser pulse: (a) $\tau = 0.5$, (b) $\tau = 3.5$, (c) $\tau = 6.5$, (d) $\tau = 9.5$. The axes are scaled using the dimensionless coordinates $\xi = x\omega_0/c$, $\nu = y\omega_0/c$, and $\zeta = z\omega_0/c$. Maps of the ratio $\tilde{\eta} = (\eta - \eta_{\text{min}}) / (\eta_{\text{max}} - \eta_{\text{min}})$ are plotted using a colormap ranging from red to purple: high (respectively low) values of $\tilde{\eta}$ correspond to red (respectively purple). The quantities η_{max} and η_{min} are the maximum and minimum values of η at the instant τ considered, respectively.

IV. CONCLUSIONS

Let us sum up the main results of this work as follows:

- (i) For the first time, we were able to derive the system of governing equations describing the evolution of the electric field and charge density during the propagation of three-dimensional extremely short electromagnetic pulses through an array of semiconductor CNTs, taking into account the heterogeneity of the field along the direction parallel to the axis of the nanotubes (see Eqs. (6), (9), and (10));
- (ii) Our study demonstrates the possibility of stable propagation of the three-dimensional bipolar electromagnetic pulses, a.k.a. breathers, through an array of CNTs;
- (iii) Electromagnetic pulses propagating through the nanotubes array induce a redistribution of the electron

density throughout the sample, which may potentially lead to useful and practical applications in the field of nanoelectronics.

ACKNOWLEDGMENTS

A. V. Zhukov and R. Bouffanais are financially supported by the SUTD-MIT International Design Centre (IDC). M. B. Belonenko acknowledges a support from the Russian Foundation for Fundamental Research. The authors are grateful to Dr. Nicola Bougen-Zhukov for her assistance with the figures preparation. This paper is dedicated to Maria Zhukova, who always inspired AVZ to do something really creative.

- ¹P. J. F. Harris, *Carbon Nanotubes and Related Structures: New Materials for the Twenty-First Century* (Cambridge University Press, 1999).
- ²S. A. Maksimenko and G. Ya. Slepyan, *J. Comm. Tech. Electron.* **47**, 235 (2002).
- ³S. A. Maksimenko and G. Ya. Slepyan, in *Handbook of Nanotechnology. Nanometer Structure: Theory, Modeling, and Simulation* (SPIE Press, Bellingham, 2004).
- ⁴S. A. Akhmanov, V. A. Vysloukh, and A. S. Chirkin, *Optics of Femtosecond Laser Pulses* (AIP, New York, 1992).
- ⁵M. B. Belonenko, E. V. Demushkina, and N. G. Lebedev, *J. Russ. Laser Res.* **27**, 457 (2006).
- ⁶M. B. Belonenko, E. V. Demushkina, and N. G. Lebedev, *Phys. Solid State* **50**, 383 (2008).
- ⁷M. B. Belonenko, E. V. Demushkina, and N. G. Lebedev, *Tech. Phys.* **53**, 817 (2008).
- ⁸M. B. Belonenko, E. V. Demushkina, and N. G. Lebedev, *Russ. J. Phys. Chem. B* **2**, 964 (2008).
- ⁹N. N. Yanyushkina, M. B. Belonenko, N. G. Lebedev, A. V. Zhukov, and M. Paliy, *Int. J. Mod. Phys. B* **25**, 3401 (2011).
- ¹⁰M. B. Belonenko, A. S. Popov, N. G. Lebedev, A. V. Pak, and A. V. Zhukov, *Phys. Lett. A* **375**, 946 (2011).
- ¹¹B. A. Malomed, D. Mihalache, F. Wise, and L. Torner, *J. Opt. B: Quantum Semiclassical Opt.* **7**, R53 (2005).
- ¹²Ya. V. Kartashov and B. A. Malomed, *Rev. Mod. Phys.* **83**, 247 (2011).
- ¹³M. B. Belonenko, S. Yu. Glazov, N. G. Lebedev, and N. E. Meshcheryakova, *Phys. Solid State* **51**, 1758 (2009).
- ¹⁴M. B. Belonenko, N. G. Lebedev, and A. S. Popov, *JETP Lett.* **91**, 461 (2010).
- ¹⁵M. B. Belonenko, A. S. Popov, and N. G. Lebedev, *Tech. Phys. Lett.* **37**, 119 (2011).
- ¹⁶A. S. Popov, M. B. Belonenko, N. G. Lebedev, A. V. Zhukov, and M. Paliy, *Eur. Phys. J. D* **65**, 635 (2011).
- ¹⁷A. S. Popov, M. B. Belonenko, N. G. Lebedev, A. V. Zhukov, and T. F. George, *International Journal of Theoretical Physics, Group Theory and Nonlinear Optics* **15**, 5 (2011).
- ¹⁸E. G. Fedorov, A. V. Zhukov, M. B. Belonenko, and T. F. George, *Eur. Phys. J. D* **66**, 219 (2012).
- ¹⁹A. V. Zhukov, R. Bouffanais, M. B. Belonenko, and E. G. Federov, *Mod. Phys. Lett. B* **27**, 1350045 (2013).
- ²⁰M. B. Belonenko and E. G. Fedorov, *Phys. Solid State* **55**, 1333 (2013).
- ²¹H. Leblond and D. Michalache, *Phys. Rev. A* **86**, 043832 (2012).
- ²²M. B. Belonenko, S. Yu. Glazov, and N. E. Meshcheryakova, *Semiconductors* **44**, 1211 (2010).
- ²³L. D. Landau, E. M. Lifshitz, and L. P. Pitaevskii, *Electrodynamics of Continuous Media*, 2nd ed. (Elsevier, Oxford, 2004).
- ²⁴L. D. Landau and E. M. Lifshitz, *The Classical Theory of Fields*, 4th ed. (Butterworth-Heinemann, Oxford, 2000).
- ²⁵E. M. Epshtein, *Fiz. Tverd. Tela (Leningrad)* **19**, 3456 (1976).
- ²⁶Yu. S. Kivshar and B. A. Malomed, *Rev. Mod. Phys.* **61**, 763 (1989).
- ²⁷S. V. Kryuchkov and G. A. Syrodoev, *Sov. Phys. Semicond.* **24**, 708 (1990).
- ²⁸J. W. Thomas, *Numerical Partial Differential Equations—Finite Difference Methods* (Springer-Verlag, New York, 1995).